Constraining *qqtt* operators from four-top production: a case for enhanced EFT sensitivity *

Cen Zhang(张岑)[1)]

Institute of High Energy Physics, Chinese Academy of Sciences, Beijing 100049, China

Abstract: Recently, experimental collaborations have reported $\mathcal{O}(10)$ upper limits on the signal strength of four-top production at the LHC. Surprisingly, we find that the constraining power of four-top production on the *qqtt* type of operators is already competitive with the measurements of top-pair production, even though the precision level of the latter is more than two orders of magnitude better. This is explained by the enhanced sensitivity of the four-top cross section to *qqtt* operators, due to multiple insertion of operators in the squared amplitude, and to the large threshold energy of four-top production. We point out that even though the dominant contribution beyond the standard model comes from the $\mathcal{O}(C^4/\Lambda^8)$ terms, the effective field theory expansion remains valid for a wide range of underlying theories. Considering the possible improvements of this measurement with higher integrated luminosity, we believe that this process will become even more crucial for probing and testing the standard model deviations in the top-quark sector, and will eventually provide valuable information about the top-quark properties, leading to significant improvements in precision top physics.

Keywords: Top quark, LHC, effective field theory

PACS: 14.65.Ha, 13.85.Hd **DOI:** 10.1088/1674-1137/42/2/023104

1 Introduction

As a top-quark factory with more than six million top-quark pairs produced in Run-I and much more to expect in the future, the LHC is an ideal place to probe top-quark properties. In proton-proton collisions, most top quarks are produced in $t\bar{t}$ pairs. Single top production has the second largest cross section, about one third that of $t\bar{t}$. More recently, associated production modes such as $t\bar{t}$+X and single t+X, where X is a gauge boson or the Higgs boson, have also been extensively studied. These are the main channels that are now pushing top-quark physics into a precision era [1].

Attention has also been paid to the four-top production mode, $pp \to tt\bar{t}\bar{t}$, which, despite its tiny rate (≈ 9 fb [2, 3]) in the standard model (SM), i.e. five orders of magnitude lower than $t\bar{t}$ production (832 pb, [4, 5]), is particularly sensitive to new physics. It has been noticed that the total rate of this process can be enhanced significantly in many scenarios beyond the standard model (BSM) [6–17]. This can be due to the direct production of new resonant states which subsequently decay into tops, or to the contribution from contact four-top operators, which rises as the energy grows. These operators are not directly constrained by other processes at the tree level, and therefore the four-top channel may be the first place to see their effects.

Nevertheless, a comprehensive model-independent study of four-top production in the context of the standard model effective field theory (SMEFT) approach [18–20] has not yet appeared in the literature. This is not surprising. The SMEFT framework aims to probe indirect effects from BSM models that are beyond the direct reach of the LHC. These effects are expected to show up as relatively small deviations from the SM prediction, and therefore the most powerful approach is to combine all available precision measurements and perform global analyses. In the top-quark sector, such analyses are often based on the most precise ones, such as top-pair and single-top cross sections and distributions, branching ratio measurements, and recently also on associated production modes such as $t\bar{t}Z$ and $t\bar{t}\gamma$, see e.g. Refs. [21, 22] for a recent global fit. Four-top production, on the other hand, is still far from being precise. The process has been searched for in a series of experimental reports [23–32], and the best upper limit from Ref. [30] is about 4.6 times

Received 22 August 2017, Published online 18 January 2018

∗ Supported by the 100-talent project of Chinese Academy of Sciences

1) E-mail: cenzhang@ihep.ac.cn

the SM signal. Naively, one would not expect an $\mathcal{O}(10)$ upper bound to provide competitive information with respect to all the other precise measurements, except for the four-top operators that are not directly probed elsewhere.

The goal of this work is to demonstrate that this is not the case. For a very important class of operators, namely the contact four-fermion interactions with two top quarks and two light quarks, *qqtt*, we will show that the four-top process, with only a $\mathcal{O}(10)$ upper bound, is as powerful as $t\bar{t}$ measurements with a percentage error. This constraining power is due to an enhanced sensitivity of four-top production, which comes from the fact that its cross section can depend on up to the fourth power of the operator coefficients, which scales like $(CE^2/\Lambda^2)^4$, where E is the energy of the process, and C/Λ^2 is the coefficient of an *qqtt* operator. Given the large energy scale related to this process, and the current limits on the coefficient C/Λ^2, the factor $(CE^2/\Lambda^2)^4$ significantly enhances the sensitivity of the four-top process to the *qqtt* operators. We will also show that the validity of SMEFT and its perturbativity can be guaranteed by imposing an analysis cut on the center of mass energy of the process at a few TeV, without reducing the enhancement factor too much, and thus the resulting constraints apply to BSM theories that live above this energy scale, if certain assumptions are made to justify the omission of operators at dim-8 and higher.

For comparison, we also consider the $t\bar{t}$ observables at the LHC, and study the corresponding exclusion limit on the same class of operators. These observables have been incorporated in a global fit by the authors of Refs. [21, 22]. In this work, however, the approach we follow is quite different, mainly because we are interested in the enhancement effect of higher powers of CE^2/Λ^2. Even in $t\bar{t}$ measurements, the squared term from dim-6 operators cannot be neglected with the current precision, and therefore instead of the four linear combinations of *qqtt* operators used in Refs. [21, 22] (defined in Ref. [33]), we will have to include the complete set of 14 *qqtt* operators. A global fit, including the main cross section and asymmetry measurements, as well as a differential cross section measurement, will be performed to derive the global constraints in these 14 directions. These constraints will then be compared with those from the four-top production in the same directions. For the latter process, we will also consider the impact of including the full set of *tttt* type four-fermion operators, which might be generated together with the *qqtt* operators, when heavy mediator particles in the full theory are integrated out. Note that RG-induced constraints are also available on the *qqtt* operators [34], but they are typically considered as indirect constraints.

In this work, our numerical approach is fully based on the MadGraph5_aMC@NLO framework [3]. We use NNPDF3.0 parton distribution functions (PDF) [35]. A UFO model [36] that contains all 14 *qqtt* operators and 4 *tttt* operators is generated using the FeynRules package [37]. All calculations are done at the leading order (LO). For the four-top production, we assume that a SM K-factor of about 1.4 [2, 3] at the next-to-leading order (NLO) can also be applied to the operator contributions. This might not be a good approximation (see Ref. [38] for an example), but is the best we can do given that the NLO predictions for all *qqtt* operators are not yet available[1)]. The corresponding theoretical error at NLO is about $\sim$30%, much smaller than the experimental errors, and so it will be neglected throughout. Similarly, for the top-pair production mode, we always rescale the cross sections to the state-of-the-art theory predictions, except for the asymmetries, where the SM contribution is an NLO effect, while those from the four-fermion operators are from LO. We therefore only use the LO asymmetries from the dim-6 contributions.

Regarding the experimental limits on the four-top process, we will only consider those on the SM four-top production signal strength. This implies that the SM signal shape is always assumed. Ideally, an experimental analysis tailored to SMEFT operators, with various cuts on the center-of-mass energy to ensure the validity of the effective theory expansion, would be the best for our purpose. This, however, has not been done for the *qqtt* operators. If one naively applies the bound on the SM cross section, the limits on BSM will be more conservative, as in general the effective operators lead to harder energy distributions. This is indeed the case for the four-top operators, as has been considered in the experimental analyses in Refs. [25–28]. Furthermore, applying the upper bound of the total cross section on the fiducial cross section below some center-of-mass energy cut to ensure the SMEFT validity will also make the results conservative. Still, even these conservative constraints on *qqtt* operator coefficients already compete with those from $t\bar{t}$ measurements, so they are sufficient for the goal of this work. One should keep in mind that further improvements from the experimental side are possible.

The paper is organized as follows. In Section 2 we present the relevant dim-6 operators in this work. In Section 3 we explain the enhanced sensitivity of the four-top process, and discuss the validity range of the EFT. We compare the constraining powers of the four-top and $t\bar{t}$ cross sections in Section 4. Section 5 is devoted to a global fit using $t\bar{t}$ measurements, which will be compared with the fully marginalized constraints from four-top cross section. In Section 6 we conclude.

1) An NLO implementation of the four-fermion top operators based on the MadGraph5_aMC@NLO framework is in progress [39].

2 The four-fermion operators

In this work we are interested in the four-fermion operators that involve two top quarks and two light quarks. This is an important class of operators, as they are common in BSM models where new heavy states couple to both $t\bar{t}$ and $q\bar{q}$, or $q\bar{t}$ and $t\bar{q}$ currents.

Assuming an $\mathrm{U}(2)^{3(u,d,q)}$ flavor symmetry for the first two generations, the full set of $qqtt$ operators at dim-6 can be written as follows

$$\mathcal{O}_{Qq}^{(8,3)} = \left(\bar{Q}_L\gamma_\mu T^a\tau^i Q_L\right)\left(\bar{q}_L\gamma^\mu T^a\tau^i q_L\right) \quad (1)$$
$$\mathcal{O}_{Qq}^{(8,1)} = \left(\bar{Q}_L\gamma_\mu T^a Q_L\right)\left(\bar{q}_L\gamma^\mu T^a q_L\right) \quad (2)$$
$$\mathcal{O}_{td}^{(8)} = \left(\bar{t}_R\gamma_\mu T^a t_R\right)\left(\bar{d}_R\gamma^\mu T^a d_R\right) \quad (3)$$
$$\mathcal{O}_{tu}^{(8)} = \left(\bar{t}_R\gamma_\mu T^a t_R\right)\left(\bar{u}_R\gamma^\mu T^a u_R\right) \quad (4)$$
$$\mathcal{O}_{tq}^{(8)} = \left(\bar{t}_R\gamma_\mu T^a t_R\right)\left(\bar{q}_L\gamma^\mu T^a q_L\right) \quad (5)$$
$$\mathcal{O}_{Qd}^{(8)} = \left(\bar{Q}_L\gamma_\mu T^a Q_L\right)\left(\bar{d}_R\gamma^\mu T^a d_R\right) \quad (6)$$
$$\mathcal{O}_{Qu}^{(8)} = \left(\bar{Q}_L\gamma_\mu T^a Q_L\right)\left(\bar{u}_R\gamma^\mu T^a u_R\right) \quad (7)$$
$$\mathcal{O}_{Qq}^{(1,3)} = \left(\bar{Q}_L\gamma_\mu \tau^i Q_L\right)\left(\bar{q}_L\gamma^\mu \tau^i q_L\right) \quad (8)$$
$$\mathcal{O}_{Qq}^{(1,1)} = \left(\bar{Q}_L\gamma_\mu Q_L\right)\left(\bar{q}_L\gamma^\mu q_L\right) \quad (9)$$
$$\mathcal{O}_{td}^{(1)} = \left(\bar{t}_R\gamma_\mu t_R\right)\left(\bar{d}_R\gamma^\mu d_R\right) \quad (10)$$
$$\mathcal{O}_{tu}^{(1)} = \left(\bar{t}_R\gamma_\mu t_R\right)\left(\bar{u}_R\gamma^\mu u_R\right) \quad (11)$$
$$\mathcal{O}_{tq}^{(1)} = \left(\bar{t}_R\gamma_\mu t_R\right)\left(\bar{q}_L\gamma^\mu q_L\right) \quad (12)$$
$$\mathcal{O}_{Qd}^{(1)} = \left(\bar{Q}_L\gamma_\mu Q_L\right)\left(\bar{d}_R\gamma^\mu d_R\right) \quad (13)$$
$$\mathcal{O}_{Qu}^{(1)} = \left(\bar{Q}_L\gamma_\mu Q_L\right)\left(\bar{u}_R\gamma^\mu u_R\right) \quad (14)$$

where Q_L represents the left-handed doublet for the 3rd generation, and q_L, u_R and d_R represent the 1st and the 2nd generation quarks. The operators are summed over the first two generations, but we omit the flavor indices. Other four-fermion operators are excluded by the flavor symmetry.

For later convenience we have written the 14 operators in the form of a top-quark vector current (color singlet or octet) contracted with a light-quark vector current. Their contributions to both $q\bar{q}\to t\bar{t}$ and $q\bar{q}\to tt\bar{t}\bar{t}$ are independent of each other. One can also count the 14 degrees of freedom in a more physical way:

1) Both the light and the heavy quark currents can be either left- or right-handed. This gives 4 degrees of freedom.

2) The light quark can be up/charm or down/strange. This leads to 8 degrees of freedom in total.

3) $\mathrm{SU}(2)_L$ symmetry requires that $u_Lu_Lt_Rt_R$ and $d_Ld_Lt_Rt_R$ interactions have the same coefficient. This reduces the number of degrees of freedom to 7.

4) With two possible color structures, i.e. singlet and octet, the total number of degrees of freedom is 14.

In the $t\bar{t}$ process, the cross section can be written as a quadratic function of 14 operator coefficients:

$$\sigma=\sigma_{\rm SM}+\sum_i\frac{C_i}{\Lambda^2}\sigma_i+\sum_{i\le j}\frac{C_iC_j}{\Lambda^4}\sigma_{ij} \quad (15)$$

If one truncates the function and keeps only the interference term, then the 8 color-singlet operators, Eqs. (8)-(14), do not give any contribution at the LO. Furthermore, without information from the decay of the tops, the LLLL (LLRR) interactions cannot be distinguished from the RRRR (RRLL) operators. Therefore only 4 degrees of freedom can be observed [33], which significantly simplifies the analysis. However, the current limits on the operator coefficients C/Λ^2 indicate that the dim-6 squared terms are not negligible, and so the full set of 14 operators needs to be included in $t\bar{t}$ production. The four-top production mode is similar, and in particular, there the dominant terms may come from the fourth power of dim-6 coefficients.

Fortunately, as we will see in Section 4, the SMEFT analysis with all 14 operators can be simplified by observing that these operators can be divided into three categories according to the flavor of the light quarks, without any interference effect across:

1. u_R:
$$\mathcal{O}_{tu}^{(8)},\mathcal{O}_{tu}^{(1)},\mathcal{O}_{Qu}^{(8)},\mathcal{O}_{Qu}^{(1)}; \quad (16)$$
2. d_R:
$$\mathcal{O}_{td}^{(8)},\mathcal{O}_{td}^{(1)},\mathcal{O}_{Qd}^{(8)},\mathcal{O}_{Qd}^{(1)}; \quad (17)$$
3. q_L:
$$\mathcal{O}_{Qq}^{(8,3)},\mathcal{O}_{Qq}^{(8,1)},\mathcal{O}_{Qq}^{(1,3)},\mathcal{O}_{Qq}^{(1,1)},\mathcal{O}_{tq}^{(8)},\mathcal{O}_{tq}^{(1)}. \quad (18)$$

Furthermore, the operators in the first two categories can be easily related to those in the last category by parity. This implies that one analysis with 14 operators can be simplified into two independent analyses, each with only 4 operators, from the 1st or the 2nd category, and parity can be used to derive results for the 3rd category. This is one of the reasons for choosing the operator basis given by Eqs. (1)–(14). As we will see, this simplification is very important for analyzing the four-top production process, as there the cross section is a quartic function of 14 operators, with a large number of interference terms.

We also consider the operators that consist of four top quarks. These four-top operators are important because unlike the $qqtt$ ones, they are bound to be generated as long as there are BSM particles coupled to the top quark. The four-top production is the first process to directly probe them (see, for example, discussions in Refs. [7, 8, 16, 40]). In this work we will also provide constraints on these operators. Note that our main goal is to derive constraints on the $qqtt$ operators, however, reliable constraints need to be obtained by marginalizing over other operators that enter the same process. This is the main reason to study the contribution from four-top

operators, as we want our conclusion to be independent of their sizes.

Five such operators exist in the so-called Warsaw basis [41]:

$$\mathcal{O}_{qq}^{(1)(3333)},\mathcal{O}_{qq}^{(3)(3333)},\mathcal{O}_{uu}^{(3333)},\mathcal{O}_{qu}^{(1)(3333)},\mathcal{O}_{qu}^{(8)(3333)}. \quad (19)$$

Among them only four are independent in four-top production, which we define as

$$\mathcal{O}_{QQ}^{(+)}\equiv\frac{1}{2}\mathcal{O}_{qq}^{(1)(3333)}+\frac{1}{2}\mathcal{O}_{qq}^{(3)(3333)}, \quad (20)$$

$$\mathcal{O}_{tt}\equiv\mathcal{O}_{uu}^{(3333)}, \quad (21)$$

$$\mathcal{O}_{Qt}^{(1)}\equiv\mathcal{O}_{qu}^{(1)(3333)}, \quad (22)$$

$$\mathcal{O}_{Qt}^{(8)}\equiv\mathcal{O}_{qu}^{(8)(3333)}, \quad (23)$$

while the remaining degree of freedom is chosen as

$$\mathcal{O}_{QQ}^{(-)}\equiv\frac{1}{2}\mathcal{O}_{qq}^{(1)(3333)}-\frac{1}{2}\mathcal{O}_{qq}^{(3)(3333)}, \quad (24)$$

with no contribution to the process.

These four-top operators in general interfere with the other *qqtt* operators in four-top production. For a complete analysis, one will have to consider each category in Eqs. (16)-(18) together with these four operators. The parity relation still holds, under which $C_{QQ}^{(+)}$ and C_{tt} are exchanged (neglecting contributions initiated by two b quarks).

The relation between our four-fermion operator basis and the more standard basis, i.e. the Warsaw basis in Ref. [41], is given in Appendix A.

Finally, we briefly explain the notation used in this work. The coefficients of dim-6 operators are denoted as C/Λ^2. One should keep in mind that the C and Λ individually do not have any physical meaning. Only their combination is a physical quantity. We define

$$\tilde{C}_i\equiv\frac{C_i(1\ \text{TeV})^2}{\Lambda^2} \quad (25)$$

so that constraints on SM deviations can be conveniently quoted in terms of $\tilde{C}$. The values of $\tilde{C}$ are constrained by experiments and are model-independent. On the other hand, we use Λ_{NP} to denote the characteristic scale at which the new physics resides. This is not a model-independent quantity, but it is useful for defining the range of validity of the EFT expansion, which requires $E<\Lambda_{NP}$, where E is the typical energy transfer in the process of interest.

3 Sensitivity and EFT validity

To briefly explain the sensitivity of the four-top process to four-fermion *qqtt* operators, let us take $\mathcal{O}_{tu}^{(8)}$ as an example. This operator represents a contact interaction between a color octet right-handed up-quark current and a color octet right-handed top-quark current. We first consider the $t\bar{t}$ process. $t\bar{t}$ measurements so far impose the tightest bounds on *qqtt* operators. The LO cross section at 8 TeV, rescaled to the next-to-next-to-leading order (NNLO) prediction, including the resummation of next-to-next-to-leading logarithmic (NNLL) soft gluon terms [4, 5], is numerically given by (in pb):

$$252.9+2.94\tilde{C}_{tu}^{(8)}+0.411\tilde{C}_{tu}^{(8)2}. \quad (26)$$

Using the combined ATLAS and CMS measurement on $t\bar{t}$ inclusive cross section [42], we find the following bounds

$$-11.8<\tilde{C}_{tu}^{(8)}<4.6 \quad (27)$$

at the 95% confidence level (CL). Interestingly, both the upper and the lower limits on $\tilde{C}_{tu}^{(8)}$ come only from the upper bound of the cross section. In particular for the lower limit $\tilde{C}_{tu}^{(8)}=-11.8$, the squared term in Eq. (26) already dominates over the interference.

As we have mentioned in the introduction, it is this same effect, i.e. the dominance of terms with higher powers in $\tilde{C}$, that enhances the EFT sensitivity of four-top production. In particular, at LO, the 14 *qqtt* type operators can be inserted at most twice in the amplitude. The squared amplitude at LO is thus a quartic function with 14 arguments:

$$O=O_{\text{SM}}+\sum_i\frac{C_i}{\Lambda^2}O_i+\sum_{i\le j}\frac{C_iC_j}{\Lambda^4}O_{ij}+\sum_{i\le j\le k}\frac{C_iC_jC_k}{\Lambda^6}O_{ijk}+\sum_{i\le j\le k\le l}\frac{C_iC_jC_kC_l}{\Lambda^8}O_{ijkl}, \quad (28)$$

where O represents any observable. Focusing again on $\mathcal{O}_{tu}^{(8)}$, without worrying about EFT validity for the moment, the LO total cross section is (in fb)

$$6.1+0.10\tilde{C}_{tu}^{(8)}+0.081\tilde{C}_{tu}^{(8)2}+0.016\tilde{C}_{tu}^{(8)3}+0.0048\tilde{C}_{tu}^{(8)4}. \quad (29)$$

The CMS search presented in Ref. [30] gives an upper bound on the signal strength of the four-top process, $\mu<4.6$. Naively applying this result to Eq. (29), we find the following constraints

$$-8.8<\tilde{C}_{tu}^{(8)}<7.1, \quad (30)$$

which are already complementary to the previous constraints from $t\bar{t}$. Note, however, that when these constraints are saturated, it is the $\tilde{C}_{tu}^{(8)4}$ term that gives the dominant contribution. Had we truncated Eq. (29) to, say, the linear term in $\tilde{C}_{tu}^{(8)}$, the resulting constraints would have been more than one order of magnitude worse. This implies that the four-top process has an enhanced sensitivity to *qqtt* operators, due to the contribution from higher power terms in $\tilde{C}$, and this is why such a process with only a $\mathcal{O}(10)$ upper bound on its signal strength can beat the $t\bar{t}$ measurement with a precision at the percentage level. Note that which term dominates depends on the size of $\tilde{C}_{tu}^{(8)}$, and is therefore related to the current experimental bounds. The quartic term dominates if $|\tilde{C}_{tu}^{(8)}|>4.1$, while the quadratic one

dominates if $1.2<|\tilde{C}_{tu}^{(8)}|<4.1$. As the experimental constraints continue to improve in the future, the situation might change. Also note that a similar effect, i.e. the dominance of the quadratic term, has been observed in multijet production [43].

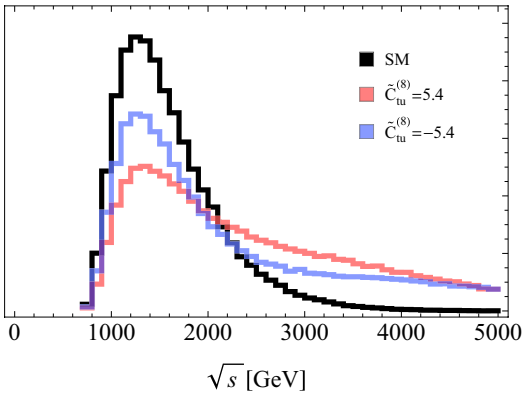

Fig. 1. (color online) Center-of-mass energy distribution of four-top production, normalized, to illustrate the typical energy scale of this process. Results are shown for the SM case and for $\tilde{C}_{tu}=\pm 5.4$.

The above observation, however, leads to two questions: why the high power terms dominate, and whether the SMEFT expansion is still valid. The first question is mostly explained by the large energy scale related to the four-top process. The threshold of four-top production is $4m_t\approx 690$ GeV. Most signal events have a typical center of mass energy of $\gtrsim\mathcal{O}(1)$ TeV, depending on the value of the operator coefficients, as illustrated in Figure 1. The series in Eq. (29) comes from multiple insertion of the four-fermion effective interaction in the squared amplitude, and by power counting each insertion corresponds to a factor of CE^2/Λ^2, where E is the characteristic energy of the process. The current constraints on C/Λ^2 then imply that

$$\frac{CE^2}{\Lambda^2}>1 \tag{31}$$

and so terms with the highest power in C/Λ^2 are supposed to dominate[1)]. Note that this is not true for all operators. For example, another important operator that enters both $t\bar{t}$ and four-top production channels is the top-quark chromo-magnetic dipole operator,

$$\mathcal{O}_{tG}=y_t g_s(\bar{Q}\sigma^{\mu\nu}T^A t)\tilde{\phi}G^A_{\mu\nu}. \tag{32}$$

The contribution of this operator does not scale as CE^2/Λ^2 because of the Higgs vev. It is also better constrained by $t\bar{t}$ in the gg initiated channel. As a result, the four-top limit on C_{tG} cannot compete with the one from the $t\bar{t}$ measurement, and so we will not consider it in this work.

The second question is more crucial. The fact that higher power terms in Eq. (29) dominate seems to imply the breakdown of the EFT expansion, as one could ask whether the contributions from dim-8 and higher operators can be safely ignored in an EFT expansion, given that they scale the same way in $1/\Lambda$ as the higher-power terms in Eq. (29). Therefore the validity of the EFT expansion itself needs to be justified. Here to make things clear, it is important to distinguish between two kinds of "expansions". The EFT expansion comes from integrating out heavy degrees of freedom at the energy scale Λ_{NP} (to be distinguished from the non-physical Λ), a procedure whose legitimacy is related to $E/\Lambda_{NP}<1$. This means that for a given process one could always truncate the SMEFT Lagrangian at a certain dimension [44]. This is however different than the "expansion" in Eq. (29), which instead comes from multiple insertion of dimension-six effective interaction and squaring the amplitude. In this case the "expansion parameter" is $CE^2/\Lambda^2>1$. However, this second "expansion" is not related to EFT validity, and is strictly speaking not even an expansion: there are no more terms after the fourth power of CE^2/Λ^2 (at LO, with on-shell tops and no further radiations), so there is no need to truncate. Simply put, when $CE^2/\Lambda^2>1$ is allowed by experimental constraints, one should only truncate the expansion in the dimension of operators, but keep all terms in a series of CE^2/Λ^2. The relative theory error due to neglecting higher order terms is then controlled by $E^2/\Lambda^2_{NP}<1$, instead of $CE^2/\Lambda^2>1$.

As a simple example of the above argument, it has been discussed in Refs. [45, 46] that in a wide class of BSM models with strongy couplings, the contribution from dim-8 operators is subleading with respect to dim-6 squared terms, without invalidating the EFT expansion. An explicit example has been given in Ref. [46], where a $2\to 2$ scattering process is considered. The SM contribution is of order g^2_{SM}, while a dimension-six operator coming from integrating out the heavy mediator can be as large as $g^2_* E^2/\Lambda^2_{NP}$, where g_* is the BSM coupling of the mediator to the SM particles. We have

$$\frac{C}{\Lambda^2}\sim\frac{g^2_*}{\Lambda^2_{NP}}. \tag{33}$$

If the coupling g_* is much larger than the SM coupling g_{SM} (which is often the case when experimental constraints are saturated, if Λ_{NP} is kept larger than E), the

1) Eq. (31) with $E\approx\sqrt{s}$ tends to overestimate the effective contribution. The reason is that the energy transfer at the effective vertices is often less than $\sqrt{s}$. The only configuration where the energy transfer is equal to $\sqrt{s}$ is the case where the two initial quarks enter the same effective vertex, which then produces $t^*\bar{t}\to t\bar{t}t\bar{t}$, but in this case the squared amplitude can depend on at most two powers of Cs/Λ^2. Still, in this process either $(\frac{CE^2}{\Lambda^2})^4$ with $E\lesssim\sqrt{s}$ or $(\frac{Cs}{\Lambda^2})^2$ represents a large factor.

BSM contribution dominates the SM contribution when $(g_*/g_{SM})^2E^2/\Lambda_{NP}^2>1$, and similarly the BSM squared term dominates over the interference term between SM and BSM. The EFT expansion is still valid if $E/\Lambda_{NP}<1$, because a $2\to2$ scattering at the tree level can be enhanced at most by g_*^2, and therefore no g_*/g_{SM} factor exists between dimension-six and dimension-eight operators. In general the validity of the EFT expansion is not spoiled by a large g_*, or a large C/Λ^2, because the maximum power of g_* in a given process is fixed. As a physics case, in reality the LHC sensitivities to the triple-gauge-boson couplings are completely dominated by dim-6 squared contributions, while the global EFT analyses can be performed without including dim-8 operators [47, 48].

In four-top production the situation is similar. The $q\bar{q}\to tt\bar{t}\bar{t}$ amplitude can be enhanced at most by $g_*^4E^4/\Lambda_{NP}^4\sim(CE^2/\Lambda^2)^2$, and the cross section by $(CE^2/\Lambda^2)^4$, as shown in for example Fig. 2(a). Upon integrating out the heavy mediators, the amplitude in the EFT is described by Fig. 2(b), i.e. with two insertions of dimension-six operators. However, the crucial difference here is that truncating the higher-dimensional operators is not guaranteed as in a $2\to2$ process. At this point, model dependent assumptions on the underlying theories are indispensable for further discussion. For simplicity, and following Ref. [46], let us assume that the underlying theory is characterized by one scale Λ_{NP} and one coupling g_*, and that the power counting in the EFT is given by [49]

$$\mathcal{L}_{\rm EFT}=\frac{\Lambda_{NP}^4}{g_*^2}\mathcal{L}\left(\frac{D_\mu}{\Lambda_{NP}},\frac{g_*H}{\Lambda_{NP}},\frac{g_*f_{L,R}}{\Lambda_{NP}^{3/2}},\frac{gF_{\mu\nu}}{\Lambda_{NP}^2}\right). \tag{34}$$

Higher dimensional operators can be constructed in different ways. One can use the first expansion parameter in Eq. (34), D_μ/Λ_{NP}, to increase the dimension without changing the field content. This is like expanding a heavy mediator propagator $(p^2-M^2)^{-1}=-M^{-2}(1+p^2/M^2+p^4/M^4+\ldots)$, where $M\approx\Lambda_{NP}$, so the expansion parameter is simply E^2/Λ_{NP}^2. In this case neglecting higher-dimensional operators is justified. Alternatively, one can also use $g_*f_{L,R}/\Lambda_{NP}^{3/2}$ or g_*H/Λ_{NP} to increase the dimension, and the expansion parameter is enhanced by g_*, so higher-dimensional operators have a chance to contribute more. This, however, cannot be done repetitively, because at some point the operator will contain more than six fields and become irrelevant (assuming LO amplitude dominates, and neglecting the vev, as we are interested in the high-energy regime). The question is where to stop this g_* enhanced expansion. Note that the dim-6 contribution is dominated by amplitudes like Fig. 2(b) which already scale like $g_*^4E^4/\Lambda_{NP}^4$. The first relevant operator that is enhanced by g_*^4 is a dim-10 operator, $g_*^4f^6D$, whose contribution scales like $g_*^4E^6/\Lambda_{NP}^6$. This is still subdominant. For illustration we give an example in Fig. 2(c) and (d), in a model with a heavy mediator with coupling strength g_*. Note that the two-to-four process can be enhanced at most by g_*^4 at tree level, and a SMEFT operator that contains six fermions is at least at dim-10, because odd-dimensional operators do not exist in the SM if B and L number violating operators are ignored [50, 51]. On the other hand, dim-8 operators are enhanced at most by 3 powers of g_*. Since both the dim-8 and dim-10 contributions are less than $g_*^4E^4/\Lambda_{NP}^4$, and further enhancement with g_* beyond dim-10 is not possible without adding more particles, we conclude that, under the above assumption, truncating the SMEFT at dim-6 is justified.

It is important to keep in mind that this conclusion is model-dependent. In practice one could come up with theories with more than one scale or coupling, where the dim-8/10 contributions might be important. As a general rule, when interpreting results obtained with a dim-6 SMEFT in specific models, one always needs to check the validity of the EFT by estimating the impact of higher dimensional contributions.

It remains to be shown that the validity condition, $E/\Lambda_{NP}<1$, can be taken under control. As proposed in Ref. [46], the standard way to deal with this in a hadron collider is to apply a mass cut $M_{\rm cut}$ on the center of mass energy of the event, or some other observable that characterizes the energy scale of the process. Results of the analysis should be provided as functions of $M_{\rm cut}$. The

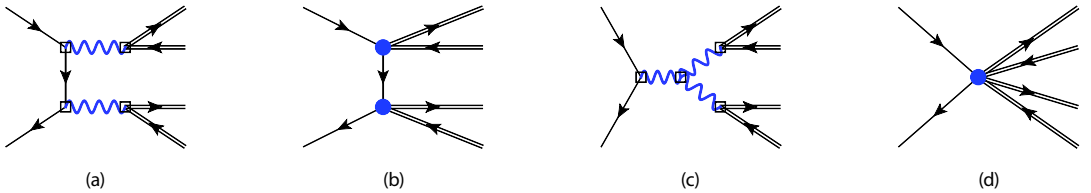

Fig. 2. (color online) The $q\bar{q}\to tt\bar{t}\bar{t}$ amplitudes that are enhanced by four powers of BSM coupling g_*. Blue lines are heavy mediators. Double lines represent the top quarks. The squares represent g_* couplings, and the blue blobs represent effective operators, coming from integrating out the mediators. Diagrams (a) and (c) describe the amplitudes in the underlying theory, while in the EFT they respectively correspond to (b) and (d). Diagrams (a) and (b) correspond to two insertions of dim-6 operators. They scale like $g_*^4E^4/\Lambda_{NP}^4$. Diagrams (c) and (d) correspond to one insertion of a dim-10 operator. They scale like $g_*^4E^6/\Lambda_{NP}^6$.

SMEFT approach is then valid if the results are interpreted with BSM models that satisfy $\Lambda_{NP} > M_{\rm cut}$, and theory errors due to missing higher dimensional terms can be estimated by $M^2_{\rm cut}/\Lambda^2_{NP}$. As we have mentioned in the introduction, since the experimental search is not carried out with this kind of strategy, we will simply apply various $M_{\rm cut}$ of order a few TeV on the center-of-mass energy in our cross section calculation. The resulting fiducial cross sections are required to be less than the upper bound set on the SM total cross section, which then gives conservative constraints.

To illustrate how well the SMEFT can reproduce the full theory prediction below $M_{\rm cut}$, we have considered an explicit model with a heavy vector mediator particle of mass M_V and width $M_V/(8\pi)$ that couples to the right-handed quark currents. The coupling corresponds to $\tilde{C}^{(1)}_{tu}=-4$ and $\tilde{C}_{tt}=-2$[1]. The invariant mass distributions for $M_V=5$, 6, 8 TeV and for the EFT case (equivalent to $M_V\to\infty$) are compared in Fig. 3. Note that the SM contribution is very small compared with the EFT, as the latter is dominated by the dim-6 quartic contributions. Dim-8 and higher-dimensional contributions are, however, subleading, as illustrated by the differences between the EFT curve and the explicit models. For the 5 TeV case, the cross section below $M_{\rm cut}=3$ TeV is reproduced by the EFT with about 30% error, roughly corresponding to $(M_{\rm cut}/\Lambda_{NP})^2$, as expected. For larger mediator masses the EFT approximation becomes better, which implies that the EFT validity issue will become less severe as the measurements continue to improve in the future. This example corresponds to $|CE^2/\Lambda^2|\approx 36$.

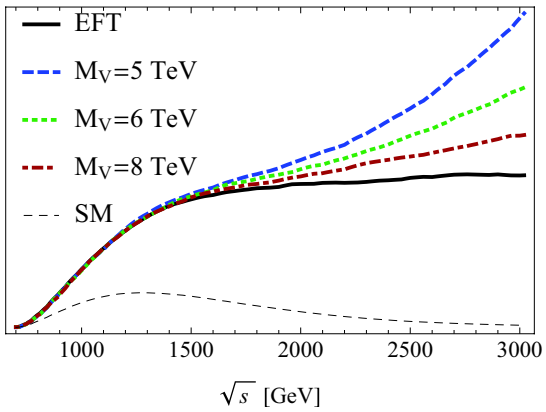

Fig. 3. (color online) Center-of-mass energy distribution of four-top production, to illustrate the validity of EFT. Results are shown for EFT, the SM, and for $M_V=5$, 6, 8 TeV respectively.

The discussion in this section is based on LO accuracy. The $qq\to tt\bar{t}\bar{t}$ amplitude can go beyond the fourth power of CE^2/Λ^2, if loop corrections are important. In this case dim-8 operators are also needed for a consistent theory prediction, as in general two dim-6 operators can mix with a dim-8 one. Given the precision level of the process, we simply impose the following perturbativity condition

$$\frac{CE^2}{(4\pi)^2\Lambda^2} < \frac{CM^2_{\rm cut}}{(4\pi)^2\Lambda^2} < 1. \tag{35}$$

to make sure the loop corrections due to additional insertion of effective operators are not important. This will be checked for typical values of $M_{\rm cut}$. A related issue is that jets in the final state may allow additional powers of CE^2/Λ^2. As an example, we find that the $tt\bar{t}\bar{t}jj$ cross section depends on $\tilde{C}^{(8)6}_{tu}$, with a coefficient of 5.6×10^{-5} fb. This term is less important than the $\tilde{C}^{(8)4}_{tu}$ term if $\tilde{C}^{(8)}_{tu}<9$, consistent with the perturbativity condition for $M_{\rm cut}\approx 4$ TeV. Finally, additional powers of CE^2/Λ^2 may come from non-top operators, if on-shell top quarks are not strictly required. We will simply assume that these operators are more likely to be constrained by other non-top measurements.

4 The signal process

The cross section of four-top production is a quartic function of the 14 $qqtt$ operator coefficients. Such a function in general has $C^4_{14+4}=3060$ terms. Numerically determining this function will then require at least 3060 independent simulations at different parameter space points, which is huge amount of work. Fortunately, as we have explained in Section 2, the procedure can be simplified into two steps. The first step is to determine the cross section as functions of operators in the first two categories, separately, which requires a minimum of only $C^4_{4+4}+C^4_{4+4}-1=139$ independent simulations. The second is to derive the cross section as a function of operators in the third category, with the help of parity. Namely, if one imposes

$$C^{(8)}_{Qu}=C^{(8)}_{Qd},\quad C^{(1)}_{Qu}=C^{(1)}_{Qd}, \tag{36}$$

then the cross section is invariant under the following transformation

$$C^{(a)}_{Qu}=C^{(a)}_{Qd} \quad\Leftrightarrow\quad C^{(a)}_{tq}, \tag{37}$$

$$C^{(a)}_{\substack{tu\\td}} \quad\Rightarrow\quad C^{(a,1)}_{Qq}\pm C^{(a,3)}_{Qq}, \tag{38}$$

$$C^{\left(a,\frac{1}{3}\right)}_{Qq} \quad\Rightarrow\quad \frac{1}{2}\left(C^{(a)}_{tu}\pm C^{(a)}_{td}\right), \tag{39}$$

where $a=1,8$. Using these relations, the dependence on the third category operators can be derived from that of the first two.

1) When Λ_{NP} is large, it may seem that these values would require a large coupling strength which is not compatible with our assumption on the width. However it is always possible to obtain large values of $\tilde{C}$ without using a very strong coupling by arranging more than one particles, or using group factors from a large representation, etc.

When the four-top operators are included, in each category one has to consider together the 4 *qqtt* operators and the 4 *tttt* operators. The *tttt* operators can be inserted only once in the amplitude, if the *qqtt* operators are not inserted twice in the same amplitude. This increases the total number of independent terms to 705, which is still manageable. The parity relations can still be used to derive the dependence on the third category operators, provided that

$$C_{QQ}^{(+)} \Leftrightarrow C_{tt} \tag{40}$$

is added to Eqs. (37)-(39).

Following the procedures described above, to determine the dependence of the four-top cross section on the 14 *qqtt* and 4 *tttt* operator coefficients, we have randomly generated $\sim\mathcal{O}(1000)$ points in the parameter space, and computed the cross section at these points, applying $M_{\rm cut}=2$, 3, 4 TeV respectively. These points are uniformly distributed roughly within the experimentally allowed region of the coefficients. Results are then fitted to the polynomial described above. We have checked that the prediction of the fitted function at all these sampled points agree with the simulation within 3% error.

With this function we are ready to evaluate the constraining power of the signal process, and compare the constraints from four-top production with those obtained from $t\bar{t}$ measurements. For this purpose we first consider single measurements of the $t\bar{t}$ total cross sections at the LHC, including:

- 8 TeV ATLAS, $\sigma=242.9\pm8.8$ pb [52],
- 13 TeV CMS, $\sigma=888^{+33}_{-34}$ pb [53].

Corresponding theoretical predictions at NNLO+NNLL are taken from Refs. [4, 5]. For the four-top production, we consider the current upper bound with signal strength $\mu<4.6$ [30], applying the $M_{\rm cut}=3$ TeV cut on the center-of-mass energy. We further consider the projection for an integrated luminosity at 300 fb^{-1}, $\mu<1.87$, estimated by Ref. [32], and apply $M_{\rm cut}=2$ TeV and 3 TeV respectively.

In Fig. 4 we show the resulting constraints at 95% confidence level, for the operators in the first category (i.e. those that couple to u_R), with two operators turned on at a time. Results for the other two categories are similar and are given in Appendix B. From these plots, our observations are the following:

1) Current constraints from four-top production already provide competitive constraints (black dashed lines), which are close to, and in some cases better than, the constraints from the 13 TeV $t\bar{t}$ measurement with only a 4% error (green dashed lines).

2) The 8 TeV $t\bar{t}$ measurement so far gives better constraints (green shaded area), but even these will be superseded in the future by an improved search/measurement of four-top production at 300 fb^{-1} luminosity with a projected $\mu<1.87$ upper bound (black solid lines), assuming $M_{\rm cut}=3$ TeV.

3) Lowering $M_{\rm cut}$ to 2 TeV will give somewhat looser constraints (blue solid lines), but results can be applied to more underlying models where the BSM scales are not so heavy. On the other hand, increasing this cut can further improve the constraints.

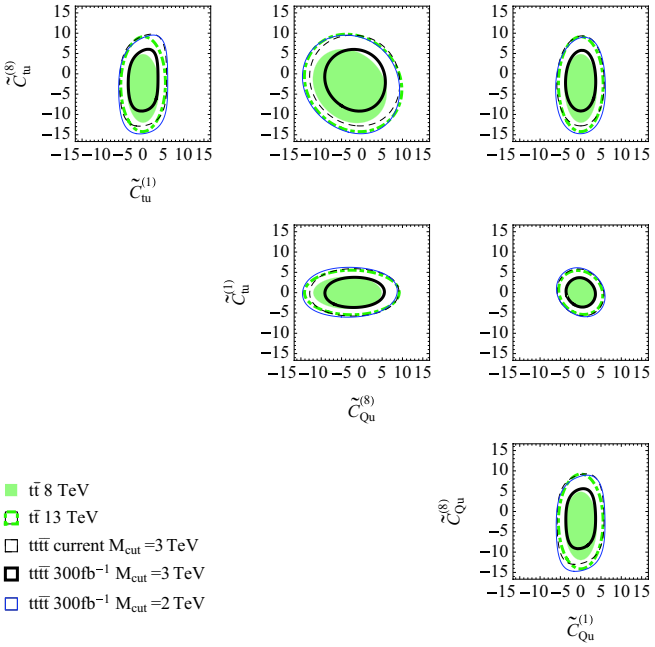

Fig. 4. (color online) Constraints from four-top cross section and individual $t\bar{t}$ cross section measurements, on the operator coefficients in the first category ($\tilde{C}_{tu}^{(8)}$, $\tilde{C}_{tu}^{(1)}$, $\tilde{C}_{Qu}^{(8)}$, $\tilde{C}_{Qu}^{(1)}$), assuming two coefficients to be nonzero at a time.

It is important to point out that the $t\bar{t}$ measurement is limited by systematic errors, and further improvements with higher luminosity is difficult. On the other hand, there is still a lot of room for the four-top search/measurement to be improved in the future. Our results indicate that, in the near future, the four-top process could even take place and provide more crucial information on *qqtt* operators. One should keep in mind that this requires a relatively large cut, $M_{\rm cut}\gtrsim2\sim3$ TeV, to be applied in the analysis, so only the BSM models that live above ~3 TeV are subject to these new constraints. This is, however, not a drawback from the SMEFT point of view, because new states below this energy scale are likely to be excluded by explicit resonance searches [1].

5 Global fit

In the previous section we have shown that the future four-top measurement can have a better sensitivity

to four-fermion operators compared with individual $t\bar{t}$ cross section measurements. However, $t\bar{t}$ production is such an important process that it has been measured extensively at many different energies (Tevatron, LHC 7, 8, 13 TeV) and in many different ways (cross section, asymmetries, distributions, etc.) A global fit of all available measurements thus provides the best available limits so far. In this section we will investigate whether the four-top process can add useful information to the global top measurement program.

The recent global fit performed by the authors of Refs. [21, 22] has included the four-fermion operators. The fit is based on four linear combinations of their coefficients, called $C^{1,2}_{u,d}$, which are the only independent degrees of freedom at the dim-6 interference level [33]. However, the theoretical set up in this work is different, in that we expect that the dim-6 squared terms can dominate given the current bounds. This has been confirmed by, for example, a fit for four-fermion operators in Ref. [54], where this dominance has been interpreted as the SMEFT being invalid. However, as explained in Section 3, in this work we distinguish the CE^2/Λ^2 expansion from the true EFT expansion E^2/Λ^2_{NP}, and in any case we expect higher powers of CE^2/Λ^2 to dominate in four-top production and to enhance its sensitivity to BSM. The actual EFT validity is then guaranteed by the assumption $\Lambda_{NP} > M_{\rm cut} \sim$ a few TeV, which is more than enough for most $t\bar{t}$ measurements.

In light of the above considerations, the fit we will perform is different to the previous ones, in that the dim-6 squared terms as well as the interference between two dim-6 operators will be fully incorporated. We will have to abandon the $C^{1,2}_{u,d}$ language, as this simplification breaks down at the dim-6 squared level. Furthermore, the color-singlet operators cannot be neglected due to the vanishing interference term. The fit will then include 14 independent operators. A complete analysis including every existing measurement is certainly beyond the scope of this work. Given that the goal is to evaluate the relative constraining powers of $t\bar{t}$ and four-top production, we will follow the approach in Ref. [54], where the most relevant measurements on cross sections and asymmetries have been included. The most recent LHC 13 TeV cross section measurements will be added as well. Furthermore, unlike Ref. [54], we shall also consider the differential m_{tt} distribution measurement to constrain the possible shape change from four-fermion operators [16]. In Table 1 we list the measurements that will be used in our fit, together with the corresponding SM predictions. We believe these observables represent the most sensitive ones to $qqtt$ operators that have been measured so far.

For simplicity, we only consider the SM prediction uncertainties as theoretical uncertainties. We add the theoretical and experimental errors in quadrature, and when the errors are not symmetric, we take the larger one for both sides. We further assume all uncertainties are uncorrelated, except for the theory ones that come from the same prediction. The fit for the m_{tt} distribution should be considered at most as a "toy fit" given that correlations between different bins are not available from the experimental report. We have dropped the last bin due to the normalization constraint. A K-factor rescaling will not improve the normalized distribution. For this reason, we use LO prediction and consider various theory errors. The scale uncertainty is from the variation of μ_R and μ_F by a factor of 2. The PDF uncertainty is taken from the envelope of three PDFs, including the NNPDF [35], MMHT [55], and CT14 [56] PDF sets with their own uncertainty bands. We have checked that the differences between LO and NLO predictions are within these errors.

A χ^2 is constructed based on the information in Table 1, to derive the 95% CL limits on operator coefficients. These limits are compared with the projection of four-top measurement at 300 fb^{-1}. Some results are shown in Fig. 5, with two operators turned on at a time. Our observations are the following:

1) In general, with a 3$\sim$4 TeV cut, constraints from the four-top cross section are very similar to those from m_{tt} measurement (black dashed vs blue and red lines). In rare cases they are complementary.

2) In most cases, combining the $t\bar{t}$ inclusive measure-

Table 1. Measurements used in the global fit, with corresponding theory predictions and uncertainties.

	SM prediction	measurement
cross section, Tevatron 1.96 TeV, CDF+D0	$7.35^{+0.26}_{-0.33}$ pb [4]	7.60±0.41 pb [57]
cross section, LHC 8 TeV, ATLAS+CMS	$252.9^{+13.3}_{-14.5}$ pb [4]	241.5±8.5 pb [42]
cross section, LHC 13 TeV, CMS	832^{+40}_{-45} pb [5]	888^{+33}_{-34} pb [53]
cross section, LHC 13 TeV, ATLAS	832^{+40}_{-45} pb [5]	818^{+36}_{-36} pb [58]
A_{FB}, Tevatron 1.96 TeV, CDF+D0	0.095 ± 0.007 [59]	0.128 ± 0.025 [60]
A_C, LHC 8 TeV, ATLAS	0.0111 ± 0.0004 [61]	0.009 ± 0.005 [62]
A_C, LHC 8 TeV, CMS	0.0111 ± 0.0004 [61]	0.0033 ± 0.0042 [63]
m_{tt} distribution, LHC 8 TeV, ATLAS	MadGraph5_aMC@NLO+PYTHIA6 [64]	Ref. [65]

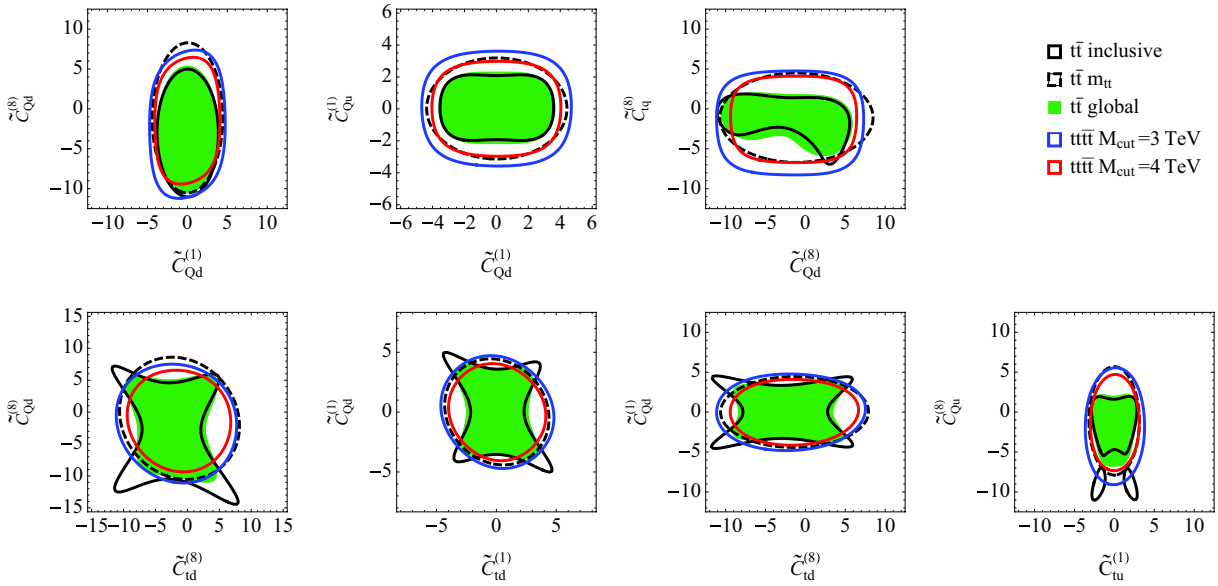

Fig. 5. (color online) Selected results for $t\bar{t}$ global fit, compared with projected constraints from the four-top production at high luminosity, at 95% CL. Black solid and dashed contours represent constraints from $t\bar{t}$ inclusive measurements (i.e. cross sections and asymmetries) and m_{tt} differential measurement respectively. The green shaded area is the combined result. Constraints from $tt\bar{t}\bar{t}$ with $M_{\rm cut}$=3, 4 TeV are given by the blue and red curves separately.

ments, i.e. the cross sections and asymmetries, provides the most constraining limits, as expected. This is illustrated by the three plots in the first row in Fig. 5. Results from m_{tt} differential measurements and four-top cross sections provide slightly weaker bounds. The $t\bar{t}$ global fit, including cross sections, asymmetries, and m_{tt}, is indicated by the green shaded area.

3) Exceptions are the directions that are not effectively constrained by asymmetry measurements. In this case both m_{tt} differential measurements and the four-top cross section provide better limits. These cases are illustrated in the second row in Fig. 5. The diagonal directions roughly correspond to flat directions between the LLLL/RRRR operators and the LLRR/RRLL operators, whose contributions to A_{FB} and A_C have the opposite sign. The asymmetry measurements thus do not provide useful information in these directions. When two operators are turned on, there can be four such directions, as the dominant contributions come from the dim-6 squared terms. This can be seen in Fig. 5, second row. Clearly, in these cases both the m_{tt} and the four-top measurements help to further improve our reach in SM deviations.

Given that the four-top measurement provides almost the same information as the m_{tt} differential cross section, we do not expect the four-top to give better constraints than a global fit on the $qqtt$ operators. It is, however, a valuable addition to the precision top physics at the LHC, given that the m_{tt} distribution is already one of the most sensitive observables to four-fermion operators. In particular, in directions that are not sensitive to asymmetry measurements, information from the four-top process is useful. For this reason we expect that marginalized constraints from a $t\bar{t}$ global fit and those from the four-top process are comparable. However, to really confirm this point in a model-independent way, we need to take into account the four-top operators given in Eqs. (20)-(23), to derive the fully marginalized constraints from the four-top process. Naively, one would expect that further marginalizing over the additional $tttt$ operators would make the constraints on $qqtt$ operators weaker. We will show that, while this is indeed the case, the effect is not large enough to qualitatively change our conclusion.

For illustration, in Fig. 6 we present the constraints on four-top operators. These are marginalized over other four-top operators, but not the $qqtt$ operators. The current constraints are derived using $M_{\rm cut}$=3 TeV, while the projected ones for 300 fb^{-1} are given with $M_{\rm cut}$=2, 3, 4 TeV, respectively. The constraints are more conservative than those directly extracted from a tailored experimental analysis, e.g. Ref. [28]. This is expected because we assume a SM signal shape and only use the cross section below $M_{\rm cut}$. Also note that even for the most constraining limits, the dim-6 squared contribution already dominates over the interference. For this reason, including these operators in our analysis should not significantly affect the constraints on the other 14 $qqtt$ operators.

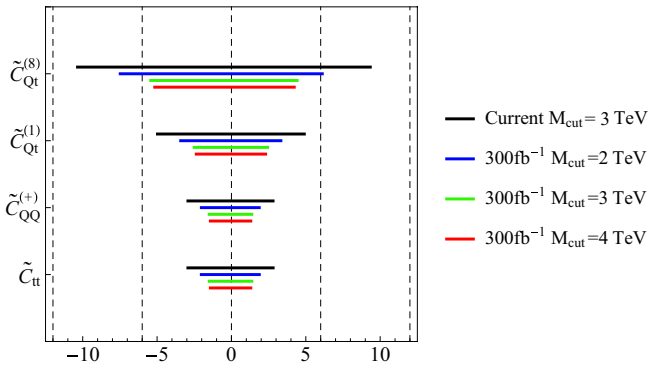

Fig. 6. (color online) Marginalized constraints on four-top operators, using the current bound as well as the projection for 300 fb^{-1}, for several $M_{\rm cut}$ values.

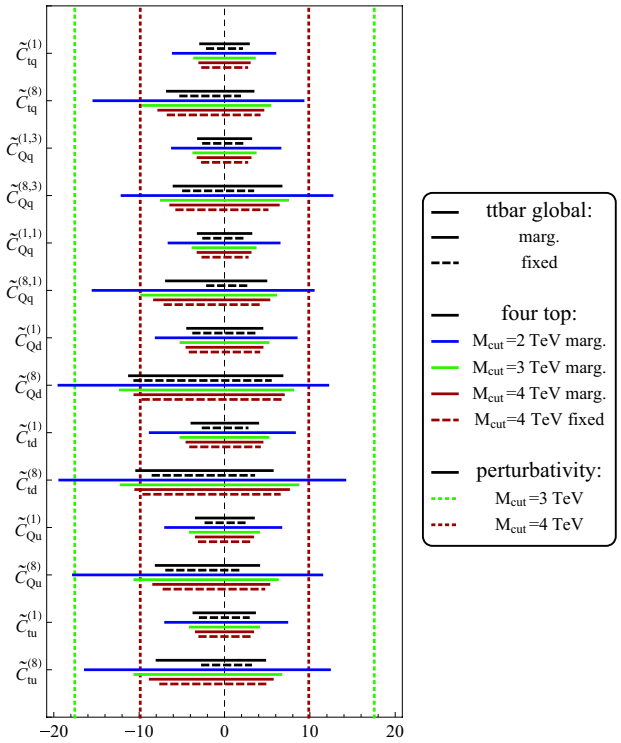

Fig. 7. (color online) Fixed (i.e. one operator at a time) and fully marginalized (i.e. all other operators floated) constraints for all $qqtt$ operators, from four-top measurement and from $t\bar{t}$ measurements, at 95% CL. The $t\bar{t}$ constraints are from our global fit, while the four-top constraints are from the 300 fb^{-1} projection. Different $M_{\rm cut}$ values are applied. Perturbativity bounds are derived from Eq. (35).

In Fig. 7 we present the most important results of this work: a comparison of fixed (i.e. one operator at a time) and fully marginalized (i.e. all other operators floated) constraints for all $qqtt$ operators, from the four-top measurement and from the $t\bar{t}$ measurements. The $t\bar{t}$ constraints are from our global fit, including cross sections, asymmetries, and m_{tt} distribution, while the four-top constraints are from the 300 fb^{-1} projection, $\mu<1.87$, with different $M_{\rm cut}$ values applied. Perturbativity in the EFT requires Eq. (35) to hold. This leads to an upper bound of $|\tilde{C}|<39$, 18, and 9.9 respectively for $M_{\rm cut}=2$, 3, 4 TeV. The latter two are shown in Figure 7 by the vertical dotted lines.

We can see that, while the $M_{\rm cut}=2$ TeV results are worse, the $M_{\rm cut}=3$, 4 TeV marginalized constraints are in general as good as those from the $t\bar{t}$ global fit. This agrees with our previous expectation: the $t\bar{t}$ global analysis gives better individual constraints, thanks to the asymmetry measurements, while the four-top production is very helpful in directions that are not sensitive to these measurements. Marginalizing over additional four-top operators does not significantly change our results. In fact, for the four-top process the difference between individual limits and fully marginalized ones is in general not very large (see the difference between the red solid and the red dashed lines), which implies that the cross section is dominated by the $(CE^2/\Lambda^2)^4$ terms, while the interference between different operators or with the SM is small. We want to emphasize that the four-top constraints obtained in this work are in general conservative, and in practice better results can be expected from a tailored experimental analysis. For example, in the case of the four-t_R operator $\mathcal{O}_{tt}$, by assuming the spectrum via the EFT model, the constraints can be enhanced by a factor of ~ 2 compared with assuming the SM signal shape [28]. One could imagine that a similar factor applies also to $qqtt$ operators, and in this case the four-top cross section could even be more constraining than a $t\bar{t}$ global fit. In addition, in the future combining searches/measurements in different channels could further improve the reach.

Perturbativity in general is not a problem for $M_{\rm cut}=2$, 3 TeV, while for 4 TeV some of the marginalized constraints start to approach or even go beyond the perturbative limit. Unitarity gives further constraints. Following Ref. [50], we find that the following constraints

$$C_i^{(1)}\frac{E^2}{\Lambda^2}\lesssim 4\sqrt{6}\pi, \tag{41}$$

$$C_i^{(8)}\frac{E^2}{\Lambda^2}\lesssim 24\sqrt{2}\pi, \tag{42}$$

apply to color singlet and octet operators respectively. These values imply that the limits obtained with $M_{\rm cut}=2\sim3$ TeV are more or less safe, while the improvements due to including events from $3\sim4$ TeV are not reliable, even though these improvements are quite small already. It should be noted that the unitarity problem with $M_{\rm cut}\approx4$ TeV is at most temporary, as the experimental precision will continue to improve. In fact, considering the possible improvements discussed in the pre-

vious paragraph, it is likely that going to 4 TeV is safe already with the assumed luminosity.

In any case, we conclude that in the near future, compared with a $t\bar{t}$ global fit, the four-top production can provide competitive constraints, due to its enhanced sensitivity to four-fermion $qqtt$ operators. Including this process in the global top-fitting program will definitely improve our reach in SM deviations in the top sector. Compared with $t\bar{t}$ inclusive measurements, which are dominated by systematic errors, high-mass $t\bar{t}$ production and four-top production have more room to improve. In the long term, they should become crucial channels that determine our final reach at the LHC.

Before concluding, we remind the reader that the cost of such an enhanced sensitivity is a relatively large value of $M_{\rm cut}$, which implies that the results are applicable only to BSM scenarios above this scale. In the long term, however, we believe that in any case new states below this energy scale are likely to be excluded by explicit resonance searches. One should also keep in mind that when these results are interpreted with explicit BSM models, it typically implies that a large BSM coupling is allowed, and so one should always check the sizes of higher dimensional operators, to make sure that the truncation of the SMEFT at dim-6 is valid.

6 Conclusion

Precision measurements are not just for precision itself. The ultimate goal is the higher reach in testing new physics and the ability to exclude deviations from the SM, and therefore sensitivity to SM deviations is crucial. An observable with an enhanced sensitivity to SM deviations, even poorly measured, may have a chance to play an important role. We have demonstrated this last point, using the four-top production process in the top EFT context. As a benchmark to assess its sensitivity, we use the top-pair production measurements for comparison. We have found that, as far as the dim-6 four-fermion operators are concerned, the current upper bound on the four-top signal strength at the $\mathcal{O}(10)$ level is already as powerful as the $t\bar{t}$ cross section measurements which have percentage level precision. Furthermore, using the projected bounds for 300 fb^{-1} at 13 TeV, the four-top measurement can even compete with a global fit using $t\bar{t}$ measurements, including the m_{tt} differential distributions. This comparison is remarkable as the four-top cross section was never considered as a precision measurement like the $t\bar{t}$ process.

The origin of the enhanced sensitivity of the four-top cross section comes from the fact the four-fermion operators can be inserted up to four times in the squared amplitude, each time with a factor CE^2/Λ^2 enhancing their contribution to the cross section. This factor can be larger than one, given the current limits on C/Λ^2, and the typical center-of-mass energy of the four top quarks produced. We have shown that the validity of the EFT, or in other words the validity of expansion in higher dimensional operators, can be controlled by $E^2 < M_{\rm cut}^2 < \Lambda_{NP}^2$, without spoiling the enhancement effect for $M_{\rm cut} \sim$ a few TeV, and that the EFT perturbativity $CM_{\rm cut}^2/\Lambda^2 < (4\pi)^2$ is also satisfied in general. The four-top measurement can thus provide useful bounds for underlying BSM models that live at a scale $\gtrsim$ a few TeV, and is therefore a valuable add to the precision top physics at the LHC, in particular, given that there is still a lot of room for this process to improve in the future. On the other hand, for BSM scenarios below a few TeV, these results may not apply, but in any case one expects that there the explicit resonant searches provide better exclusion.

For comparison purpose we have performed a global fit for the most relevant $t\bar{t}$ measurements, including a differential measurement on m_{tt}, to which the four-fermion operators are sensitive. Unlike previous studies, our fit is done including all dim-6 squared terms as well as interference effects between all 14 dim-6 operators. We have also included the four-top operators in our analysis, and have demonstrated that marginalizing over these operators does not qualitatively change our conclusion. Compared with our $t\bar{t}$ global fit, the four-top process gives comparable limits on all operator coefficients. One should, however, keep in mind that these limits are still relatively conservative, given that the upper bound on the total cross section assumes a SM signal shape, and is used regardless of the value of the $M_{\rm cut}$. We expect that future experimental analyses following the SMEFT strategy will further improve the sensitivity of this process to SM deviations.

Finally, we would like to point out that other processes can potentially have a similar enhanced sensitivity, provided that the following conditions are satisfied: 1) there are multiple heavy particles in the final state, so that the process is naturally related with a large energy scale; 2) multiple insertion of dim-6 operators is allowed, thus potentially leading to more powers of CE^2/Λ^2 enhancing the EFT contribution; and 3) the contribution of dim-6 operators goes like E^2/Λ^2, i.e. not suppressed by any mass or Higgs vev factors. Of course, the validity of EFT has to be checked carefully as one starts to approach the boundary of its applicability. Still, we hope that this study can inspire new ideas about using observables that are not so precisely measured, to further push the frontier of precision measurements in the EFT context.

CZ thanks Gauthier Durieux and Fabio Maltoni for their invaluable advice.

Appendix A

Operator basis

Here we present the relations between the coefficients of our four-fermion operators and those of the basis operators in the so-called Warsaw basis, in Ref. [41].

qqtt operator coefficients:

$$C_{Qq}^{(1,8)} \equiv C_{qq}^{(1)(i33i)} + 3C_{qq}^{(3)(i33i)}, \tag{A1}$$

$$C_{Qq}^{(3,8)} \equiv C_{qq}^{(1)(i33i)} - C_{qq}^{(3)(i33i)}, \tag{A2}$$

$$C_{Qq}^{(1,1)} \equiv C_{qq}^{(1)(ii33)} + \frac{1}{6}C_{qq}^{(1)(i33i)} + \frac{1}{2}C_{qq}^{(3)(i33i)}, \tag{A3}$$

$$C_{Qq}^{(3,1)} \equiv C_{qq}^{(3)(ii33)} + \frac{1}{6}\left(C_{qq}^{(1)(i33i)} - C_{qq}^{(3)(i33i)}\right), \tag{A4}$$

$$C_{tu}^{(8)} \equiv 2C_{uu}^{(i33i)}, \tag{A5}$$

$$C_{td}^{(8)} \equiv C_{ud}^{(8)(33ii)}, \tag{A6}$$

$$C_{tu}^{(1)} \equiv C_{uu}^{(ii33)} + \frac{1}{3}C_{uu}^{(i33i)}, \tag{A7}$$

$$C_{td}^{(1)} \equiv C_{ud}^{(1)(33ii)}, \tag{A8}$$

$$C_{tq}^{(8)} \equiv C_{qu}^{(8)(ii33)}, \tag{A9}$$

$$C_{Qu}^{(8)} \equiv C_{qu}^{(8)(33ii)}, \tag{A10}$$

$$C_{Qd}^{(8)} \equiv C_{qd}^{(8)(33ii)}, \tag{A11}$$

$$C_{tq}^{(1)} \equiv C_{qu}^{(1)(ii33)}, \tag{A12}$$

$$C_{Qu}^{(1)} \equiv C_{qu}^{(1)(33ii)}, \tag{A13}$$

$$C_{Qd}^{(1)} \equiv C_{qd}^{(1)(33ii)}; \tag{A14}$$

tttt operator coefficients:

$$C_{QQ}^{(+)} \equiv C_{qq}^{(1)(3333)} + C_{qq}^{(3)(3333)}, \tag{A15}$$

$$C_{tt}^{(1)} \equiv C_{uu}^{(3333)}, \tag{A16}$$

$$C_{Qt}^{(1)} \equiv C_{qu}^{(1)(3333)}, \tag{A17}$$

$$C_{Qt}^{(8)} \equiv C_{qu}^{(8)(3333)}, \tag{A18}$$

where on the l.h.s are the coefficients of the operators used in this work, while on the r.h.s are the coefficients of the Warsaw operators. i=1,2 is a flavor index.

Appendix B

More results

We present constraints from four-top production and $t\bar{t}$ cross section measurements, similar to Fig. 4, but for the operators in the 2nd and the 3rd categories, i.e. in Eqs. (17) and (18). They are displayed in Fig. B1 and Fig. B2, respectively.

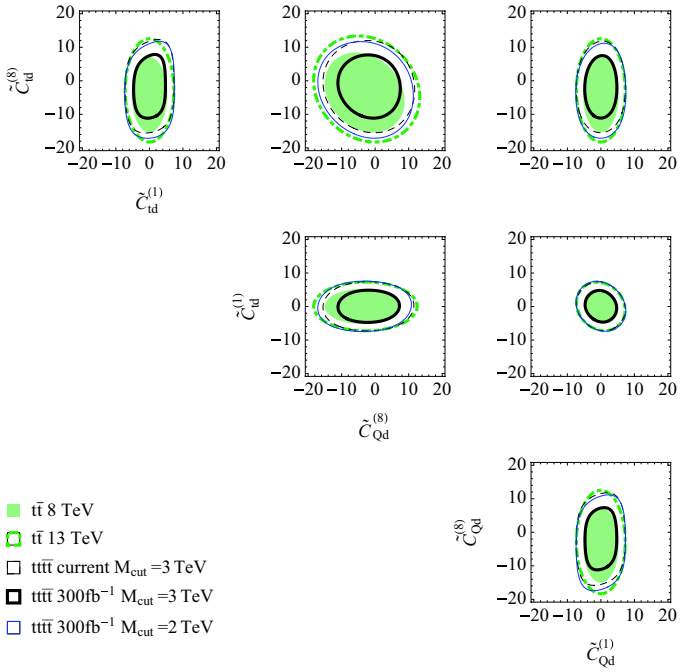

Fig. B1. (color online) Constraints from four-top cross section and individual $t\bar{t}$ cross section measurements, on the operator coefficients in the second category ($\tilde{C}_{td}^{(8)}$, $\tilde{C}_{td}^{(1)}$, $\tilde{C}_{Qd}^{(8)}$, $\tilde{C}_{Qd}^{(1)}$), assuming two coefficients to be nonzero at a time.

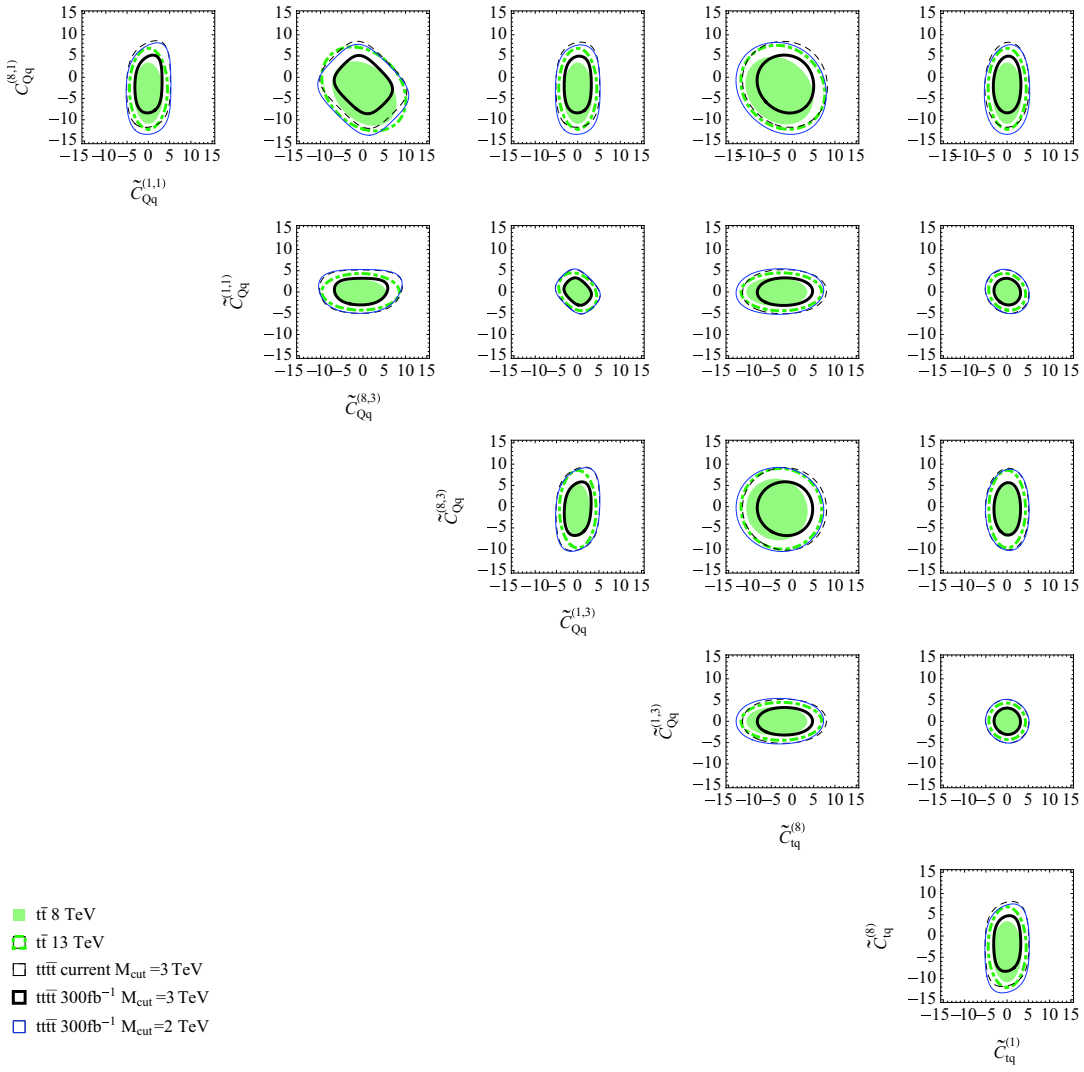

Fig. B2. (color online) Constraints from four-top cross section and individual $t\bar{t}$ cross section measurements, on the operator coefficients in the third category ($\tilde{C}_{Qq}^{(8,1)}$, $\tilde{C}_{Qq}^{(1,1)}$, $\tilde{C}_{Qq}^{(8,3)}$, $\tilde{C}_{Qq}^{(1,3)}$, $\tilde{C}_{tq}^{(8)}$, $\tilde{C}_{tq}^{(1)}$), assuming two coefficients to be nonzero at a time.

References

1 C. Patrignani et al (Particle Data Group), Chin. Phys. C, **40**(10): 100001 (2016)
2 G. Bevilacqua and M. Worek, JHEP, **1207**: 111 (2012)
3 J. Alwall et al, JHEP, **1407**: 079 (2014)
4 M. Czakon, P. Fiedler, and A. Mitov, Phys. Rev. Lett., **110**: 252004 (2013)
5 M. Czakon and A. Mitov, Comput. Phys. Commun., **185**: 2930 (2014)
6 B. Lillie, J. Shu, and T. M. P. Tait, JHEP, **0804**: 087 (2008)
7 A. Pomarol and J. Serra, Phys. Rev. D, **78**: 074026 (2008)
8 K. Kumar, T. M. P. Tait, and R. Vega-Morales, JHEP, **0905**: 022 (2009)
9 G. Cacciapaglia, R. Chierici, A. Deandrea et al, JHEP, **1110**: 042 (2011)
10 M. Perelstein and A. Spray, JHEP, **1109**: 008 (2011)
11 J. A. Aguilar-Saavedra, and J. Santiago, Phys. Rev. D, **85**: 034021 (2012)
12 L. Beck, F. Blekman, D. Dobur et al, Phys. Lett. B, **746**: 48 (2015)
13 P. S. Bhupal Dev and A. Pilaftsis, JHEP, **1412**: 024 (2014) Erratum: [JHEP, **1511**: 147 (2015)]
14 B. S. Acharya, P. Grajek, G. L. Kane et al, arXiv:0901.3367 [hep-ph].
15 T. Gregoire, E. Katz, and V. Sanz, Phys. Rev. D, **85**: 055024 (2012)
16 C. Degrande, J. M. Gerard, C. Grojean et al, JHEP, **1103**: 125 (2011)
17 Q. H. Cao, S. L. Chen, and Y. Liu, Phys. Rev. D, **95**(5): 053004 (2017)
18 S. Weinberg, Phys. Rev. Lett., **43**: 1566 (1979)
19 C. N. Leung, S. T. Love, and S. Rao, Z. Phys. C, **31**: 433 (1986)
20 W. Buchmuller and D. Wyler, Nucl. Phys. B, **268**: 621 (1986)
21 A. Buckley, C. Englert, J. Ferrando et al, Phys. Rev. D, **92**(9): 091501 (2015)

22 A. Buckley, C. Englert, J. Ferrando et al, JHEP, **1604**: 015 (2016)
23 The ATLAS Collaboration, ATLAS-CONF-2012-130
24 CMS Collaboration CMS-PAS-TOP-13-012
25 G. Aad et al (ATLAS Collaboration), JHEP, **1508**: 105 (2015)
26 The ATLAS collaboration, ATLAS-CONF-2016-013
27 The ATLAS collaboration ATLAS-CONF-2016-020
28 The ATLAS collaboration (ATLAS Collaboration), ATLAS-CONF-2016-104
29 A. M. Sirunyan et al (CMS Collaboration), Phys. Lett. B, **772**: 336 (2017)
30 A. M. Sirunyan et al (CMS Collaboration), arXiv:1704.07323 [hep-ex]
31 M. Aaboud et al (ATLAS Collaboration), arXiv:1704.08493 [hep-ex]
32 E. Alvarez, D. A. Faroughy, J. F. Kamenik et al, Nucl. Phys. B, **915**: 19 (2017)
33 C. Zhang and S. Willenbrock, Phys. Rev. D, **83**: 034006 (2011)
34 J. de Blas, M. Chala, and J. Santiago, JHEP, **1509**: 189 (2015)
35 R. D. Ball et al (NNPDF Collaboration), JHEP, **1504**: 040 (2015)
36 C. Degrande, C. Duhr, B. Fuks et al, Comput. Phys. Commun., **183**: 1201 (2012)
37 A. Alloul, N. D. Christensen, C. Degrande et al, Comput. Phys. Commun., **185**: 2250 (2014)
38 O. Bessidskaia Bylund, F. Maltoni, I. Tsinikos et al, JHEP, **1605**: 052 (2016)
39 C. Degrande, G. Durieux, F. Maltoni et al, in preparation
40 G. Servant, doi:10.3204/DESY-PROC-2010-01/251
41 B. Grzadkowski, M. Iskrzynski, M. Misiak et al, JHEP, **1010**: 085 (2010)
42 CMS Collaboration CMS-PAS-TOP-14-016
43 F. Krauss, S. Kuttimalai, and T. Plehn, Phys. Rev. D, **95**(3): 035024 (2017)
44 T. Appelquist and J. Carazzone, Phys. Rev. D, **11**: 2856 (1975).
45 A. Biekotter, A. Knochel, M. Kramer et al, Phys. Rev. D, **91**: 055029 (2015)
46 R. Contino, A. Falkowski, F. Goertz et al, JHEP, **1607**: 144 (2016)
47 A. Butter, O. J. P. Eboli, J. Gonzalez-Fraile et al, JHEP, **1607**: 152 (2016)
48 A. Falkowski, M. Gonzalez-Alonso, A. Greljo et al, JHEP, **1702**: 115 (2017)
49 A. Pomarol, Higgs Physics, in *Proceedings of the 2014 European School of High-Energy Physics (ESHEP 2014)*: edited by M. Mulders, G. Zanderigh, p.59
50 C. Degrande, N. Greiner, W. Kilian et al, Annals Phys., **335**: 21 (2013)
51 A. Kobach, Phys. Lett. B, **758**: 455 (2016)
52 G. Aad et al (ATLAS Collaboration), Eur. Phys. J. C, **74**(10): 3109 (2014) Addendum: [Eur. Phys. J. C, **76**: no. 11: 642 (2016)]
53 A. M. Sirunyan et al (CMS Collaboration), arXiv:1701.06228 [hep-ex]
54 M. P. Rosello and M. Vos, Eur. Phys. J. C, **76**(4): 200 (2016)
55 L. A. Harland-Lang, A. D. Martin, P. Motylinski et al, Eur. Phys. J. C, **75**(5): 204 (2015)
56 S. Dulat et al, Phys. Rev. D, **93**(3): 033006 (2016)
57 T. A. Aaltonen et al (CDF and D0 Collaborations), Phys. Rev. D, **89**(7): 072001 (2014)
58 M. Aaboud et al (ATLAS Collaboration), Phys. Lett. B, **761**: 136 (2016)
59 M. Czakon, P. Fiedler, and A. Mitov, Phys. Rev. Lett., **115**(5): 052001 (2015)
60 (CDF and D0 Collaborations), FERMILAB-CONF-16-386-PPD, CDF-NOTE-11206, D0-NOTE-6492.
61 W. Bernreuther and Z. G. Si, Phys. Rev. D, **86**: 034026 (2012)
62 G. Aad et al (ATLAS Collaboration), Eur. Phys. J. C, **76**(2): 87 (2016)
63 V. Khachatryan et al (CMS Collaboration), Phys. Rev. D, **93**(3): 034014 (2016)
64 T. Sjostrand, P. Eden, C. Friberg et al, Comput. Phys. Commun., **135**: 238 (2001)
65 M. Aaboud et al (ATLAS Collaboration), Phys. Rev. D, **94**(9): 092003 (2016)